RFID Grids: Part I—Electromagnetic Theory

Gaetano Marrocco

***Abstract*—The close displacement of UHF RFID tags can be considered as an electromagnetic interconnected system having specific properties. The so denoted RFID Grid includes single-chip tags in close mutual proximity or a single tag with a multiplicity of embedded microchips. A multi-port scattering framework is used to derive the macroscopic parameters governing the system response which could be optimized for the specific application. Moreover, unique features are introduced, such as the possibility to improve the power scavenging and the generation of analog identifiers and fingerprint. The last ones are electromagnetic responses independent on the position and orientation of the reader and on the nearby environment, with great relevance for Sensing and Security.**

***Index Terms*—Backscattering, coupling, grid, RFID, sensor.**

I. Introduction

THE radiofrequency identification technology (RFID) for object tagging [1] is rapidly evolving toward the "Internet of Things" [2], [3]: the convergence of a number of research disciplines (identification, real-time localization, sensor networks, pervasive computing) that enable the Internet to get into the real world of physical objects interacting with web services.

Measuring, labelling and timing of made things and humans and their mapping into the environment are expected to stimulate new context-aware services. Pleasant user experience will be planned at the workplaces, in public areas as well as in the home environment by embedding computational intelligence into the nearby environment and simplifying human interactions with everyday services.

The pervasive interconnection with things will require to deploy a multitude [4] of RFID tags, even provided with sensing capability, and to conceive new functions. RFID tags have been also hypothesized to be randomly mixed with various bulk materials to develop *amorphous* computing capability [5].

Remotely powered (passive) UHF (870-960MHZ) tags are one of the most attractive option within the multiform RFID galaxy due to low-cost, no need for maintenance, room-comparable read range and high data-rate. RFID tags are tiny computers with tiny radios and merge together both digital (the microchip data generation) and analog features (antennas and propagation phenomenology). Data transmitted back to the reader during the interrogation protocol are digitally encoded, but the strength of the backscattered power is governed in an analogical manner by the interaction with nearby objects, by the propagation modality [6], and even by the mutual position and orientation among reader and tags.

Sensing applications of passive multi-tags or multi-microchips devices are increasingly researched in the very last years. In [7] the use of a two-chip tag, embedding inertial accelerometers, was first introduced to transmit discrete motion information by the so called ID modulation. A similar concept was applied in [8] to encode the digital output of a sourced sensor by means of four tags. In [9] and [10] the multi-chip paradigm was extended to the continuous sensing of parameters. Here, the dependence of the tag antenna's electrical features on the time-variation of the physical and geometrical properties of the tagged object, was fully exploited yielding the concept of *self-sensing tags*. Finally, multiple, closely spaced, tag were used in [11] as electromagnetic field probes.

Packing many radio elements into small spaces yields an electromagnetic complex system where tags interact among themselves and with the nearby objects. In both the cases the electromagnetic properties of the data link (read distance, bit error rate, space uniformity) are affected somehow.

Most of the available papers concerning the mutual proximity of tags mainly consider the dense displacement in terms of degradation of the RFID link quality and investigate on possible mitigation solutions. Back in the 1970s, it was already shown [12] that the electromagnetic coupling between antennas in transmitting and receiving modes are different and that such a coupling may be mitigated by a proper non-linear loading at the antennas' port. More recently, the coupling mechanism involving non-linear loads has been theoretically addressed in [6] for general purpose applications, while [14] has put into evidence, by means of a combined antenna/non-linear model, the need for a multi-tag design procedure to balance the coupling effects. Rich experimentations have been presented in [15], [16] concerning stacked planes of RFID tag antennas [17]. This configuration seems to produce interference effects on readability analogous to classic reflection filters as well as phenomena of collective modulation potentially able to distort the received signals. It was moreover verified, and corroborated by theoretical models, that tags with small radar cross section are more suited for application in dense configurations. The presence of *weak spots* in linear ad multi-dimensional alignment of near field and long range tags was addressed in [18]–[20] by means of both experiments and modeling. Depending on the inter-tag spacing, the performances of the center antennas could be worse than the side antennas, due to the voltage standing wave across the array. Finally [21] recognizes, through experimentation and simulations, that microchips with larger impedance permit to achieve tag displacements more immune to the coupling effects.

In this paper the UHF *RFID grids* are fully investigated as an electromagnetic interconnected system with the purpose to ex-

Manuscript received February 02, 2010; revised August 03, 2010; accepted August 28, 2010. Date of publication January 13, 2011; date of current version March 02, 2011. This work was supported by the PRIN-2010 project.

The author is with the DISP-University of Roma Tor Vergata, 00133 Roma, Italy (e-mail: marrocco@disp.uniroma2.it).

Color versions of one or more of the figures in this paper are available online at http://ieeexplore.ieee.org.

Digital Object Identifier 10.1109/TAP.2010.2103019

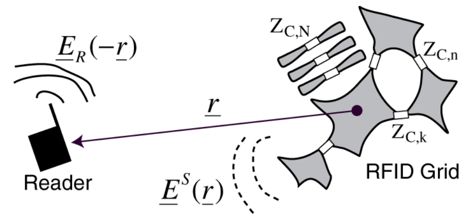

Fig. 1. Interrogating reader and RFID Grid connected to microchips of impedances $\{Z_{C,n}\}$. The reader's field $\underline{E}_R$ and the backscattered field $\underline{E}^S$ are both referred to the grid's coordinate system.

tend the usual RFID link equations to the more complex case of multi-chip configurations, deriving the expressions of realized gain, impedance matching and backscattered power and highlighting not only the principal limitation but also useful undocumented features. The term *grid* is here used to indicate a generally coupled multitude of UHF tags, including standalone tags in close mutual proximity as well as tags with a multiplicity of embedded RFID microchip transponders able to achieve advanced capabilities such as redundancy and sensing. This RFID grid is here analyzed by the electromagnetic formalism of multiport scatterers with specific care to the unique feature of the asymmetric UHF RFID communication which involves energy scavenging to wake up the microchip and then the transmission of data by backscattering modulation.

One of the most valuable achievement of the theoretical study is the concept of *analog identifier* which complements the digital identifier of a tag. This is a physical invariant deduced for an RFID grid which embeds structural properties of the specific device, as attached onto a specific object. This parameter will demonstrate to be independent on the nearby environment and may be collected by the reader from any direction. As it will be discussed next, this property could be useful to achieve non conventional sensing capabilities and to develop security fingerprints.

Finally, starting from the most general configurations, interesting properties are derived for the particular class of periodic RFID grids, such as infinite and uniform array of tags, or configuration with circular symmetry, and ready to apply formulas are given for the two-port tags.

II. Description of the System

A pictorial view of an RFID grid is sketched in Fig. 1. The grid's terminals, where microchips are connected, act as the ports of the grid. Let $Z_{C,n} = R_{C,n} + jX_{C,n}$ denote the equivalent impedance of the nth microchip in the energy-scavenging mode. As discussed later on, this impedance will be changed during the backscattering modulation. For generality $\{Z_{C,n}\}$ are assumed to be different. The reader unit interrogating the grid emits a field $\underline{E}_R$. This arrangement may represent a set of independent tags, electromagnetically coupled by proximity effects, or a unique radiating element provided with multiple independent microchips and sensors. In any case the system will be hereafter regarded as a unique electromagnetic object.

Although the presented approach is of general application, the whole formulation is specified for the UHF and higher frequency RFID systems, where the radiative field are predominant over the static field, which is instead the case of HF (13.56 MHz) and lower frequency tags.

The nth port is associated with an embedded gain $G_n(\hat{\underline{r}})$ and input resistance R_n^{in}, both evaluated when the other ports are open-circuited. Accordingly, an embedded effective length is also introduced $\underline{h}_n(\hat{\underline{r}})$. From the relationship [22] among the effective length, gain and antenna input resistance $(|h|^2 = (\lambda^2 R_{\text{in}} G)/(\eta_0 \pi))$, h_n is conveniently expressed as

$$\underline{h}_n(\hat{\underline{r}}) = \sqrt{\frac{R_n^{\text{in}} G_n(\hat{\underline{r}})}{\pi \eta_0}} \lambda \hat{\underline{h}}_n(\hat{\underline{r}}) \tag{1}$$

where $\hat{\underline{h}}_n = \underline{h}_n / |\underline{h}_n|$ is the polarization complex unitary vector and $\eta_0 = 120\pi\Omega$ is the vacuum impedance. It is worth noticing that, even in case of grids with distinct single-port tags, the effective length $\underline{h}_n$ accounts for the currents over all the conductors when only the nth port is fed and the others are kept in open circuit.

The field radiated by the reader can be easily rewritten in terms of the effective length $\underline{h}_R$ of the reader's antenna [22]

$$\underline{E}_R(-\underline{r}) = jk_0 \eta_0 I_R \frac{e^{-jk_0 r}}{4\pi r} \underline{h}_R(-\hat{\underline{r}}). \tag{2}$$

The dependence on link parameters such as the input power P_{in} through the reader's antenna and its gain G_R is made explicit by means of (1) and of the relationship between current I_R and input resistance of reader's antenna: $I_R = \sqrt{2P_{\text{in}}/R_R^{\text{in}}}$

$$\underline{E}_R(-\underline{r}) = j\sqrt{\frac{P_{\text{in}} G_R(-\hat{\underline{r}})}{2\pi} \eta_0} \frac{e^{-jk_0 r}}{R_n} \hat{\underline{h}}_R(-\hat{\underline{r}}) \tag{3}$$

with $\hat{\underline{h}}_R$ the polarization of the reader-emitted field.

III. Symbols

The most significant symbols used in the paper are here listed for reader's convenience.

$\underline{r}$	position of the reader's antenna with respect to the grid system.
G_n	gain of the RFID grid referred to the nth port.
$\tilde{G}_n$	embedded realized gain of the nth port.
$\underline{h}_n$	effective length of the grid related to the nth port.
$\underline{h}_R$	effective length of reader's antenna.
G_R	gain of the reader's antenna.
P_{in}	reader's power through the antenna.
R_R^{in}	input resistance of the reader's antenna.
p_n	power sensitivity of the nth microchip.
$\mathbf{Z}$	impedance matrix of unloaded grid.
$\mathbf{Z}_C$	diagonal matrix of port loading terminations $Z_{C,n}$.
$\mathbf{Z}_G$	grid matrix $Z + Z_C$.

$\mathbf{Y}_G$	grid admittance matrix: Z_G^{-1}.
Z_n^{in}	active input impedance at the nth grid's port.
τ_n	power transfer coefficient at nth port.
$\underline{E}_R$	electric field emitted by the reader.
V_n^{OC}	open circuit received voltage at nth grid's port.
$\mathbf{g}$	column vector of normalized port's gain.
χ_n	polarization mismatch between reader and nth grid port.
$P_{R\rightarrow Tn}$	power collected by the nth port of the grid.
$P_{R\leftarrow Tn}$	power backscatterd by the nth port toward the reader.
$\underline{E}^S$	field scattered by the grid.
$\underline{E}_n^{OC}$	field radiated by the grid when activated the nth port.
$\underline{E}_0^{OC}$	backscattered field by open circuit grid.
V_L	received backscatterd voltage on the reader's load.
$s_n^{\max}$	maximum reader's voltage due to modulation.
P_n^{to}	turn on power concerning the nth microchip.
F_n	analog identifier of the nth port.

IV. Network Representation

An RFID grid can be considered as a multi-port loaded scatterer, whose termination loads, e.g., the microchips' impedance status, are asynchronously changed to achieve the backscattering modulation. The electromagnetic properties of the direct link (the microchips scavenge power from the remote reader and are then ready to perform actions) and the reverse link (the microchips modulate their internal impedance to add information to the reflected wave) may be efficiently described by introducing an N*-port* analog of the grid, according to the mathematical formalism presented in [23], here specified for an RFID system.

With reference to Fig. 2, the N-port system collecting the interrogating electromagnetic wave is modelled by the $N \times N$ matrix $\mathbf{Z} = \mathbf{R} + j\mathbf{X}$ and by equivalent Thevenin voltage generators $V_n^{OC} = -\underline{h}_n \cdot \underline{E}_R$ which, according to (1) and (3) can be written as

$$V_n^{OC} = -j\frac{\lambda}{\pi}\sqrt{\frac{\eta_0 P_{\text{in}} G_R(-\hat{\underline{r}})}{2}}\frac{e^{-jkr}}{r} g_n \tag{4}$$

where

$$g_n = \sqrt{\frac{R_{nn} G_n(\hat{\underline{r}})\chi_n}{\eta_0}} e^{j\Phi_n(\hat{\underline{r}})} \tag{5}$$

is a normalized port's gain which groups the parameters of the grid. The polarization mismatch between the reader's field and the nth port's effective length has been written having made explicit the amplitude $\chi_n = |\hat{\underline{h}}_n \cdot \hat{\underline{h}}_R|^2$ and the phase $\Phi_n(\hat{\underline{r}}) = angle(\hat{\underline{h}}_n \cdot \hat{\underline{h}}_R)$. The open circuit input resistance at port n has been replaced by the self-resistance R_{nn} of the N-port network.

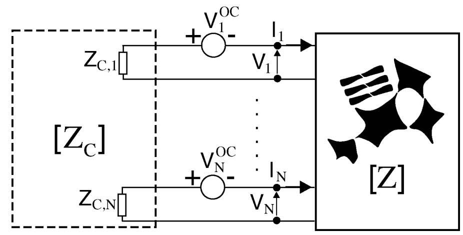

Fig. 2. Thevenin network model of the RFID-Grid where the incident field coming from the reader is accounted for by means of open circuit voltage generators V_n^{OC}. $\mathbf{Z}_C$ and $\mathbf{Z}$ are respectively the impedance matrix of the terminations and of the N-port system.

The ports' terminations are accounted for by a diagonal matrix $\mathbf{Z}_C = \mathbf{R}_C + j\mathbf{X}_C = diag(Z_{C,1}, Z_{C,2}..Z_{C,N})$ containing the microchips' impedances. The input current and voltage at the nth port are I_n V_n, respectively.

The column of port currents $\mathbf{I}$ are related to the open circuit column vector $\mathbf{V}^{OC} = [V_1^{OC}, ..V_N^{OC}]^T$ by the matrix equation $\mathbf{V}^{OC} = -(\mathbf{Z}_C + \mathbf{Z}) \cdot \mathbf{I}$ and hence

$$\mathbf{I} = -\mathbf{Y}_G \cdot \mathbf{V}^{OC} \tag{6}$$

where $\mathbf{Y}_G = \mathbf{Z}_G^{-1}$ and $\mathbf{Z}_G = (\mathbf{Z}_C + \mathbf{Z})$ are the *{grid admittance and impedance matrix*, respectively.

A. Input Impedance at Grid's Ports

The active input impedances of the RFID grid system, following the coupled array notation, are

$$Z_n^{\text{in}} = V_n / I_n = \sum_{k=1}^{n} z_{nk}\frac{I_k}{I_n} = \sum_{k=1}^{N} z_{nk}\frac{[\mathbf{Y}_G]_k \cdot \mathbf{g}}{[\mathbf{Y}_G]_n \cdot \mathbf{g}} \tag{7}$$

where $[\mathbf{Y}_G]_k$ indicates the kth row of $\mathbf{Y}_G$ and $\mathbf{g} = [g_1, ..g_N]^T$. The input active input impedance, e.g., is hence rewritten in the form

$$Z_n^{\text{in}} = \sum_{k=1}^{N} z_{nk}\frac{[\mathbf{Y}_G]_k \cdot \mathbf{g}}{[\mathbf{Y}_G]_n \cdot \mathbf{g}}. \tag{8}$$

B. Harvested Power by Grid's Microchips

The power collected at the nth port is given by $P_{R\rightarrow T,n} = (1/2)R_{C,n}|I_n|^2$. By using (6) and (4), and having introduced the *embedded realized gain* of port n

$$\tilde{G}_n = 4\eta_0 R_{C,n} \left|[\mathbf{Y}_G]_n \cdot \mathbf{g}\right|^2 \tag{9}$$

the harvested power $P_{R\rightarrow T,n}$ can be formally expressed as in the single-port case [1]

$$P_{R\rightarrow Tn} = \left(\frac{\lambda}{4\pi r}\right)^2 P_{\text{in}} G_R \tilde{G}_n. \tag{10}$$

Unlike the standard tag configuration, the roles of impedance matching, gain and polarization, are now closely confused together into the realized gain expression, and can not be generally separated.

Denoting with p_n the sensitivity of the nth microchip, the maximum activation distance for the nth port is obtained from (10) when $P_{R\to T,n} = p_n$, e.g.,

$$d_{\max,n} = \frac{\lambda}{4\pi}\sqrt{\frac{P_{\rm in}}{p_n}G_R\tilde{G}_n}. \qquad (11)$$

The embedded realized gains of the grid are therefore the parameters to be taken into account within a multi-chip antenna optimization.

V. Modulated Backscattering

According to [23], the field backscattered by the grid is

$$\underline{E}^S = \underline{E}_0^{OC} - \mathbf{E}^{OC}\cdot\mathbf{Y}_G\cdot\mathbf{V}^{OC} \qquad (12)$$

where $\underline{E}_0^{OC}$ is the field scattered by the grid when all the port are open-circuited (structural mode) and $\underline{\mathbf{E}}^{OC}$ is the row-vector of the $\underline{E}_n^{OC}$ fields radiated by the grid, considered as single port antenna, when the nth port is sourced by a unitary current and the others are open

$$\underline{E}_n^{OC} \simeq jk_0\eta_0\frac{e^{-jk_{0r}}}{4\pi r}\underline{h}_n. \qquad (13)$$

The voltage collected at the reader's load, under perfect impedance matching condition, is $V_L = -(1/2)\underline{h}_R\cdot\underline{E}^S$. By applying (1) for both reader and grids' ports and after simple mathematical manipulations the collected signal is conveniently written as

$$V_L = -\frac{1}{2}\underline{E}_0^{OC}\cdot\underline{h}_R + \frac{\eta_0}{k_0^2}G_R\sqrt{\frac{P_{\rm in}R_R^{\rm in}}{2}}(\mathbf{g}^T\cdot\mathbf{Y}_G\cdot\mathbf{g}). \qquad (14)$$

The backscattering modulation imposes that the microchip impedance at the nth port is switched between two states: $Z_C^{\rm ON}$ and $Z_C^{\rm OFF}$ and hence the corresponding received signals will be $V_L^{\rm ON}$ and $V_L^{\rm OFF}$.

The grid impedance matrix will be accordingly modulated as

$$\mathbf{Z}_G^{\rm ON/OFF} = \mathbf{Z}_G + \mathbf{M}_{(n)}^{\rm ON/OFF} \qquad (15)$$

where $\mathbf{M}_{(n)}^{\rm ON/OFF}$ is an all-zeroes matrix except for the (n,n) element:

$$\mathbf{M}_{(n)}^{\rm ON/OFF}(m,n) = \begin{cases} Z^{\rm ON/OFF} - Z_{C,n} & \text{if } n = m \\ 0 & \text{if } n \neq m. \end{cases} \qquad (16)$$

$\mathbf{Z}_G^{\rm ON/OFF}$ is hence a *one-element perturbation* of the grid impedance matrix $\mathbf{Z}_G$. The corresponding impedance matrix $\mathbf{Y}_G^{\rm ON/OFF} = (\mathbf{Z}_G + \mathbf{M}_{(n)}^{\rm ON/OFF})^{-1}$ to be introduced in (14) can be derived from un-modulated $\mathbf{Y}_G$ by using the theory of Perturbed Matrix [26]. In particular, after some manipulations (see Appendix) a compact representation is achieved to separate the modulation effect from the un-modulated response

$$\mathbf{Y}_G^{\rm ON/OFF} = \mathbf{Y}_G - \frac{Z^{\rm ON/OFF} - Z_{C,n}}{1 + Y_{G,nn}(Z^{\rm ON/OFF} - Z_{C,n})}\underset{N\times 1}{[\mathbf{Y}_G]_n^T}\cdot\underset{1\times N}{[\mathbf{Y}_G]_n}. \qquad (17)$$

As in [27], assuming modulation data encoded according to FM0 or Miller schemes and perfect-matched filter demodulation with ideal carrier recovery and the equalization at the receiver, the minimum $(s_n^{\min})$ and maximum $(s_n^{\max})$ values of input of the detector voltage can be found to be, respectively, $s_{\min} = 0$ and

$$s_n^{\max} = \frac{\left|V_L^{\rm ON} - V_L^{\rm OFF}\right|}{2} = V_0\eta_0\left|\mathbf{g}^T\cdot\left(\mathbf{Y}_G^{\rm ON} - \mathbf{Y}_G^{\rm OFF}\right)\cdot\mathbf{g}\right| \qquad (18)$$

with

$$V_0 = (k_0 r)^{-2}G_R\sqrt{P_{\rm in}R_R^{\rm in}/2}. \qquad (19)$$

Introducing the inverse of perturbed matrix in (17), the maximum received signal becomes

$$s_n^{\max} = V_0\eta_0\left|\frac{Z^{\rm OFF} - Z_{C,n}}{1 + Y_{G,nn}(Z^{\rm OFF} - Z_{C,n})} - \frac{Z^{\rm ON} - Z_{C,n}}{1 + Y_{G,nn}(Z^{\rm ON} - Z_{C,n})}\right| \cdot\left|\underset{1\times N}{[\mathbf{Y}_G]_n}\cdot\underset{N\times 1}{\mathbf{g}}\right|^2. \qquad (20)$$

The above equation shows in clear way the role of the modulation impedance, the structural properties $([\mathbf{Y}_G]_n\cdot\mathbf{g})$ and the interrogating field (inside V_0). The received signal's amplitude depends on the reader-tag distance and on the mutual reader-tag orientations since reader's and tags' gain are not isotropic.

In the particular and very common modulation choice $Z_n^{\rm ON} = Z_{C,n}$ and $Z_n^{\rm OFF} = \infty$ (or high impedance), the signal $s_n^{\max}$ reduces to

$$s_n^{\max} \simeq V_0\frac{\eta_0}{|Y_{G,nn}|}\left|[\mathbf{Y}_G]_n\cdot\mathbf{g}\right|^2 \qquad (21)$$

and introducing the expression of the embedded realized gain in (9), the following very compact form if found:

$$s_n^{\max}(\underline{r}) \simeq \frac{1}{4}V_0(r)\frac{\tilde{G}_n(\hat{\underline{r}})}{R_{C,n}|Y_{G,nn}|}. \qquad (22)$$

Without any loss of generality, above impedance switch modality will hereafter assumed for notation simplicity.

The corresponding power at the detector is hence $P_{R\leftarrow Tn} = \alpha|s_n^{\max}|^2/R_R^{\rm in}$, where the parameter α accounts for the particular demodulation used. To better appreciate the properties to be introduced in the next section, it is worth noticing that the backscattered signals $\{s_n^{\max}\}$ are strongly dependent on the whole grid admittance as well as on mutual reader-grid distance and orientation since the gain G_R and G_n are generally non isotropic. Hence, $s_n^{\max}$ data are not suited to remotely detect the variation of the chemical or physical properties of the grid, as it could be useful in sensing applications (see for instance [28]), unless the reader-grid position is kept fixed during all along the monitoring time. But even in controlled conditions, variations of the surrounding environment (e.g. a furniture is moved, a person is walking within the RFID link) will produce fluctuating data.

The intrinsic properties of the RFID grid, however, will permit to overcome this issue, disclosing new opportunities as shown in the next section.

VI. Analog Identifiers and Grid Fingerprint

The minimum power $P_{\rm in} \equiv P_n^{\rm to}$ entering into the reader's antenna for which the nth port's microchip wakes up and begins to perform actions is denoted as *turn-on power* of the nth port. In that condition the power collected by such a port equals the microchip sensitivity $P_{R\rightarrow Tn} \equiv p_n$. It is useful to combine the forward ($P_{R\leftarrow Tn}$ in (10)) and backward ($P_{R\rightarrow Tn}$) powers at turn-on in a way such to drop out the influence of distance and of the reader's and port's gains and orientation. A non-dimensional form can be hence introduced

$$F_n \equiv \frac{p_n}{2\sqrt{P_{R\leftarrow Tn}P_n^{\rm to}}} = \alpha R_{C,n}|Y_{G,nn}|. \tag{23}$$

The left side member includes power quantities which are known (p_n is declared by the microchip's manufacturer), or measurable by the reader ($P_n^{\rm to}$, $P_{R\leftarrow Tn}$). So the (23) gives a unique feature of the nth port and may be considered as a kind of *analog identifier* of the nth port. F_n is an invariant with respect to distance and to mutual orientation between reader and tag.

The set of analog identifiers of the grid, together with the digital identifier of the microchips, give the *electromagnetic fingerprint* of the multi-port system

$$\mathbf{F} = [R_{C,1}|Y_{G,11}|, \quad \cdots \quad , R_{C,N}|Y_{G,NN}|] \tag{24}$$

which, in case of identical port microchips, is proportional to the diagonal of the admittance matrix of the loaded grid. The fingerprint $\mathbf{F}(\boldsymbol{\omega})$ collected in the reader's bandwidth, is a structural property, independent on the particular interrogation modality and on the nearby environment since, in case a scattering object was present in the reader's zone, it would affect both the direct and the reverse link, and the normalization in (23) would cancel such an effect. The fingerprint generalizes to multi-chip configurations a concept recently introduced in [10] for the single-chip case.

A. RFID Fingerprint for Sensing

The RFID grid's fingerprint is expected to be greatly relevant to RFID sensing and security. Just to have an idea about the possible sensing applications of the grid's fingerprint, assume that the state of the grid is changing along with time, for instance in case geometrical or chemical properties of the surface where the grid is attached on are modified by internal or external agents, say $\boldsymbol{\Psi}$, or if the grid itself is doped with biochemical receptors. Consequently the grid fingerprint $\mathbf{F}(\boldsymbol{\Psi}(t), \omega)$ could communicate this variation to the reader, without any requirement on the interrogation position and distance. The electromagnetic design of the grid should be therefore finalized to emphasize the sensibility of the grid admittance to the external agents to be sensed. This concept poses the basis of complex self-sensing applications where the grid acts as distributed sensor, processor and communication system at a same time.

B. RFID Fingerprint for Security

Implication to Security of analog identifiers is related to physical-layer certificate of authenticity (COA) [29], [30] of the tagged object or of the tag support itself. A secure code could be produced by means of joint cryptographic processing of digital and analog identifiers of the grid, the last one being object-dependent since the grid matrix is affected by the physics of the tagged item itself. The fingerprint of grids could be made unique by introducing impurities or defects into each grid in a controllable way. In this case the electromagnetic design of the grid has to be oriented to make the fingerprint as much as stable with respect to the external agents, opposite to the requirements of the sensing applications. The promising advantage with respect to other approaches as in [29], [30] will be the simplicity in fingerprint reading, e.g., identification "on the flight," which will not require a *controllable* interrogation modality nor tag positioning, thanks to angular/distance invariance of the fingerprint itself.

VII. Periodic RFID Grids

Above general formulation takes particular simple and handy expressions when the grid's ports have equal self impedance ($Z_{nn} = Z_S$), and equal effective length along the grid's normal axis. This happens, for instance, when the RFID grid exhibits some periodicity as in the case of two identical tags placed over a plane in symmetric position or when ports are placed in circular arrangements (Fig. 3). Moreover, to have invariant polarization efficiency, the reader polarization is required to be circular.

For these cases the impedance matrix is a circulant matrix [24], e.g., a particular case of Toeplitz form ($Z_{m,n} = Z_{m-n}$) where each row vector is rotated one element to the right relative to the preceding row vector. A circulant matrix is fully specified by a single generating vector, which appears as the first row/column. The last row/column is the generating vector in reverse order. For example the $N = 4$ grid is represented by the following matrix

$$\begin{bmatrix} Z_{11} & Z_{12} & Z_{13} & Z_{14} \\ Z_{21} & Z_{22} & Z_{21} & Z_{24} \\ Z_{31} & Z_{32} & Z_{33} & Z_{34} \\ Z_{41} & Z_{42} & Z_{43} & Z_{22} \end{bmatrix} = \begin{bmatrix} Z_0 & Z_1 & Z_2 & Z_1 \\ Z_1 & Z_0 & Z_1 & Z_2 \\ Z_2 & Z_1 & Z_0 & Z_1 \\ Z_1 & Z_2 & Z_1 & Z_0 \end{bmatrix}. \tag{25}$$

For such family of matrix the sum of the elements of each row or column is a constant. The same properties are shared by the $\mathbf{Z}_G$ and $\mathbf{Y}_G$ matrices in case of equal port's impedances ($Z_{C,n} = Z_C$ for any n). This feature will be useful later on to simplify the definition of RFID-grid parameters.

If moreover the grid lays on a plane and the reader's beam is broadside with respect to the grid the forcing term g in (5)

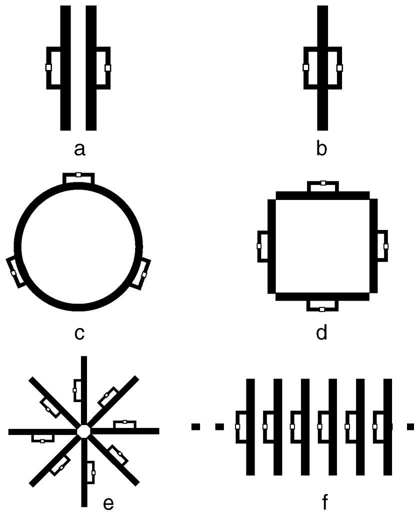

Fig. 3. Examples of periodic RFID-grids. The resulting impedance matrix has a circulant form. (a) two facing equal dipoles, (b) two-port symmetric tag, (c) three-chips tag, (d) circular alignment of four tags, (e) radial alignment of eight tags, (f) line of infinite tags.

becomes a vector with identical entries and hence the active impedances in (8) reduce to

$$Z_n^{\text{in}} = \sum_{k=1}^{N} z_{nk} \frac{\text{sum}[\mathbf{Y}_G]_k}{\text{sum}[\mathbf{Y}_G]_n}. \tag{26}$$

The embedded realized gain simplifies in

$$\tilde{G}_n = G_S \chi_S \tau_n \tag{27}$$

where G_S, χ_S are the common gain and polarization mismatch of all the ports corresponding to the broadside incidence and

$$\tau_n = 4 R_{C,n} R_S \left| \sum_{k=1}^{N} Y_{G,nk} \right|^2 \tag{28}$$

is the *embedded power transfer coefficient* associated with the nth port. The power scavenged by the nth port's microchip can be therefore rewritten in complete analogy with the one-port case, e.g.,

$$P_{R \to Tn} = \left(\frac{\lambda}{4\pi r} \right)^2 P_{\text{in}} G_R G_S \chi_S \tau_n \tag{29}$$

with full separation of impedance- and polarization-matching issues. As it will formally shown later on for the $N = 2$ case, the embedded power transfer coefficients could exceed the unit due to the constructive electromagnetic coupling among ports. Better power scavenging properties could be hence obtained in comparison with standalone tags.

In case the port impedances are all coincident ($Z_{C,n} = Z_C \ \forall n$) the properties of $\mathbf{Y}_G$ as circulant matrices apply and the corresponding active input impedances for broadside illumination in (26) are independent on the particular microchips while coincide with the sum of the row element of $\mathbf{Z}$, e.g.,

$$Z_n^{\text{in}} = \sum_{k=1}^{N} Z_{1k}, \quad \forall n \tag{30}$$

and the realized gain and power transfer coefficient are accordingly the same for each port.

A. Matching Conditions

It is worth discussing the maximum power which can be scavenged by the microchips. Under the assumption that the matrix $\mathbf{Z} + \mathbf{Z}^{*,T}$ is definite positive ('$*$' means complex conjugate), the Desoer's Theorem [25] gives the relationship between the network matrix $\mathbf{Z}$ and the termination matrix $\mathbf{Z}_C$ that is required to achieve the maximum power transfer to the $n-$ports. By the actual formalism, and since $\mathbf{Z}$ is a symmetric matrix, the Desoer condition specifies as

$$\mathbf{Z}_C \cdot \text{Re}(\mathbf{Z}) \cdot \mathbf{g} = \mathbf{Z}^* \cdot \text{Re}(\mathbf{Z}) \cdot \mathbf{g}. \tag{31}$$

The above equation admits more than a unique solution which moreover depends also on the specific querying fields. The particular solution independent on the reader-grid mutual orientation and on the radiation pattern of the reader is trivially $\mathbf{Z}_C = \mathbf{Z}^*$. However, due to the assumed form of $\mathbf{Z}_C$, this solution is feasible only if $\mathbf{Z}$ is a diagonal matrix, e.g., if the ports are decoupled. So it is more useful to consider as reference solution that one occurring in case of broadside illumination and periodic grids ($\mathbf{g}$ is a vector of equal entries). It is easy to show that (30) accordingly reduces to $Z_{C_n} = \sum_{k=1}^{N} Z_{1,k}^*$ thanks to the properties of circulant matrices (the sum of row or column elements is constant). So the maximum scavenged power requires equal microchips and from (30) the matching condition for broadside incidence can be finally rewritten as

$$Z_n^{\text{in}} = Z_C^*. \tag{32}$$

The termination impedances should be therefore equal and such to cancel the sum of self and mutual reactance.

Above condition is under-determined since there are two equations (for real and imaginary parts, respectively) and $2(N-1)$ unknowns (there are $N-1$ independent complex elements in the circulant $\mathbf{Z}$ matrix). Several options for the geometrical topologies of the grid are hence possible to achieve the best power scavenging.

The matching condition, as expected, reduces to the standard conjugate matching for the single port case. Interesting consequences on the maximum power transfer will be shown later on for the particular case of two-port grids.

It is worth noticing that the electromagnetic fingerprint of a periodic grid under broadside interrogation, and optimum impedance matching as in (32), is a vector of equal entries

$$\mathbf{F} / \left(R_C |Y_{G,11}| \right) = [1, 1, ..1]. \tag{33}$$

This function will give hence an indirect measure about the regularity of the grid and could be useful to emphasize the variation of the grid status due to the interaction with external agents.

VIII. Example of Two-Port Grid

Operative grid formulas are here specified for a two-port grid which may model the case of a two-microchip tag where a first microchip is used to transmit the identifier of the tagged object and the second to provide information about the physical status of the item. A different configuration may use both the microchips to communicate some discrete event according to the ID-modulation [7].

For the sake of simplicity a symmetric tag is assumed and hence $Z_{11} = Z_{22} \equiv Z_S$; $Z_{12} = Z_{21} = Z_M$ and

$$\mathbf{Y}_G = \frac{1}{(Z_S + Z_{C,2})(Z_S + Z_{C,1}) - Z_M^2} \cdot \begin{bmatrix} Z_S + Z_{C,2} & -Z_M \\ -Z_M & Z_S + Z_{C,1} \end{bmatrix}. \quad (34)$$

For identical port loading impedances $Z_{C,1} = Z_{C,2} \equiv Z_C$, the following equations hold

$$Z^{\text{in}} = Z_S + Z_M \quad (35)$$

$$\tilde{G}_n = G_S \chi_S \frac{4R_C R_S}{|Z_S + Z_C + Z_M|^2} \quad (36)$$

$$\tau_n = \frac{4R_C R_S}{|Z_S + Z_C + Z_M|^2} \quad (37)$$

$$s_n^{\max} = V_0 G_S \chi_S \frac{R_S}{|Z_S + Z_C|} \left| \frac{Z_S + Z_C - Z_M}{Z_S + Z_C + Z_M} \right| \quad (38)$$

$$F_n = \alpha R_{C,n} \frac{|Z_S + Z_C|}{|(Z_S + Z_C)^2 - Z_M^2|}. \quad (39)$$

Above formulas reduce to the case of one-port tag as the inter-port coupling Z_M vanishes.

Under the Hermite matching condition as in (32) the power transfer coefficients (37) is ultimately

$$\tau_{\max} = \frac{R_S}{R_C} = \frac{R_S}{R_S + R_M} \begin{matrix} < 1 & \text{if} & R_M > 0 \\ \to 1 & \text{if} & R_M \ll |R_S| \\ > 1 & \text{if} & R_M < 0 \end{matrix} \quad (40)$$

whereas improvements over the single-port case may be theoretically achieved if the mutual resistance is made negative which means that it acts as an internal generator or in other word, as discussed in [31] and [32] in the context of MIMO systems, a portion of the power scattered by each port can be recaptured by the adjacent port, particularly when the matching network is appropriately implemented. So the overall power harvested by the two-ports RFID-grid may be in principle higher than the power collected by two non-interfering tags in the same conditions (same gain and input impedance).

IX. Summary and Conclusions

This paper has introduced some properties of dense displacement of RFID devices by means of formal electromagnetic tools. The RFID grid should be considered as the physical layer implementation of an interconnected system exploiting both digital and analog features. Electromagnetic coupling is the physical mean by which the individual RFID microchips are mutually correlated since the backscattered power modulated by each microchip depends on the whole grid. It has been however demonstrated that the electromagnetic granularity of the full system, e.g., the network matrix elements, can be remotely discriminated thanks to the unique features of RFID two-ways link which involves a power wake-up threshold and coded response. The most valuable achievements of the presented theoretical formulation are listed as follows:

i) the design of an RFID grid can be performed by using the general formula in (9) for the embedded realized gain which is strictly correlated to the read range of the grid. This formula is useful for implementation within an optimization tool;

ii) in case of periodic grids, as a large array or a two-chips tag, very simplified and handy formulas (35) and (36) may be used to master the tag matching and to improve the read-range with respect to a single port tag;

iii) the analog identifier (22) and the fingerprint (23) have been introduced for the first time as invariant of the grid with many implication in sensing and security.

The RFID grid combines some of the properties of multiple-output arrays, such as the improvement of energy scavenging in comparison with coupling-free regular tags, and the distributed processing of environmental parameters. A multiplicity of sensing data, which are ambient dependent, could be collected and processed by the reader without specific requirements about reader-tag position. Based on this idea it is conceivable to develop smart self-sensing skins well suited to envelope things, plants and even body regions, which may communicate in real time their multidimensional physical history by a free sweep of the reader.

In a companion part II paper, several experimentations will be presented to verify the theory and to underline the real-world limitations of the above concepts. However, a lot of work is still needed and to fully understand the so many implications of the engineered use of a multiplicity of radio identification objects, e.g., when the RFID microchips are used not as individual devices but just as an elemental electronic component of a more complex distributed system.

Appendix

A. Details on $\mathbf{Z}_G^{\text{ON/OFF}}$ Inversion in (17)

From [26] the inverse of a $N \times N$ matrix $(\mathbf{A}+\mathbf{D})^{-1}$ where $\mathbf{D}$ is a one-element perturbing matrix $\mathbf{D}(p,q) = d$ and $\mathbf{D}(m,n) = 0$ if $p \neq m$ and $q \neq n$, can be calculated starting from $\mathbf{A}^{-1}$, as $(\mathbf{A} + \mathbf{D})^{-1} = \mathbf{A}^{-1} + \mathbf{H}$ where

$$\mathbf{H} = -\frac{d}{1 + \mathbf{A}^{-1}(q,p)d} \mathbf{A}^{-1}(*,p) \cdot \mathbf{A}^{-1}(q,*) \quad (41)$$

where $\mathbf{A}^{-1}(*,p)$ means the pth column of $\mathbf{A}^{-1}$. By setting $p = q = n$ and $d = Z_C^{\text{ON/OFF}} - Z_{C,n,}$, $\mathbf{A} = \mathbf{Z}_G$ and enforcing the matrix symmetry $(\mathbf{Z}_G^{-1}(*,p) = [\mathbf{Z}_G^{-1}(q,*)]^T$, (17) is obtained.

Acknowledgment

The author wishes to thank E. Di Giampaolo, C. Occhiuzzi and S. Caizzone for valuable discussions.

References

[1] D. M. Dobkin, *The RF in RFID: Passive UHF RFID in Practice*. Amsterdam: Elsevier, 2007.

[2] D. Preuveneers and Y. Berbers, "Internet of things: A context- awareness perspective," in *The Internet of Things: From RFID to the Next-Generation Pervasive Networked Systems*, L. Yan, Y. Zhang, L. T. Yang, and H. Ning, Eds. London: Auerbach Publications, 2008.

[3] B. Sterling, *Shaping Things*. Cambridge, MA: The MIT Press, 2006.

[4] J. Bohn and F. Mattern, “Super-distributed RFID tag infrastructures,” *Lecture Notes Comput. Sci.*, vol. 3294/2004, pp. 1–12, 2004.
[5] H. Abelson, D. Allen, D. Coore, C. Hanson, G. Homsy, T. F. Knight, F. R. Nagpal, E. Rauch, G. J. Sussman, and R. Weiss, “Amorphous computing,” *Commun. ACM*, vol. 43, no. 5, pp. 74–82, Mar. 2000.
[6] J. D. Griffin and G. D. Durgin, “Complete link budgets for backscatter-radio and RFID systems,” *IEEE Antennas Propag. Mag.*, vol. 51, no. 2, pp. 11–25, 2009.
[7] M. Philipose, J. R. Smith, B. Jiang, A. Mamishev, S. Roy, and K. Sundara-Rajan, “Battery-free wireless identification and sensing,” *IEEE Pervasive Comput.*, vol. 4, no. 1, pp. 37–45, Jan.–Mar. 2005.
[8] L. Catarinucci, R. Colella, and L. Tarricone, “A cost-effective UHF RFID tag for transmission of generic sensor data in wireless sensor networks,” *IEEE Trans Microwave Theory Tech.*, vol. 57, no. 5, pp. 1291–1296, May 2009.
[9] G. Marrocco, L. Mattioni, and C. Calabrese, “Multi-port sensor RFIDs for wireless passive sensing—Basic theory and early simulations,” *IEEE Trans. Antennas Propag.*, vol. 56, no. 8, pp. 2691–2702, Aug. 2008.
[10] G. Marrocco and F. Amato, “Self-sensing passive RFID: From theory to tag design and experimentation,” in *Proc. Eur. Microwave Conf.*, Sep. 2009, pp. 1–4.
[11] S. Capdevila, R. Serrano, A. Aguasca, S. Blanch, J. Romeu, and L. Jofre, “RFID-based flexible low-cost EM field probe,” in *Proc. IEEE Antennas Propagat. Int. Symp.*, Jul. 2008, pp. 1–4.
[12] J. P. Daniel, “Mutual coupling between antennas for emission or reception-Application to passive and active dipoles,” *IEEE Trans. Antennas Propag.*, vol. 22, no. 2, pp. 347–349, 1974.
[13] K.-C. Lee and T.-H. Chu, “Mutual coupling mechanisms within arrays of nonlinear antennas,” *IEEE Trans. Electromagn. Compat.*, vol. 47, no. 4, pp. 963–970, 2005.
[14] V. Rizzoli, A. Costanzo, M. Rubini, and D. Masotti, “Rigorous investigation of interactions between passive RFID tags by means of nonlinear/electromagnetic co-simulation,” in *Proc. 36th European Microwave Conf.*, Manchester, U.K., 2006, pp. 722–725.
[15] S. M. Seigand and D. M. Dobkin, “Multiple RFID tag plane array effects,” in *Proc. IEEE Antennas Propag. Int. Symp.*, Jul. 2006, pp. 1027–1030.
[16] D. M. Dobkin and S. M. Weigand, “UHF RFID and tag antenna scattering—Part I: Experimental results,” *Microw. J.*, vol. 49, no. 5, pp. 170–190, May 2006.
[17] D. M. Dobkin and S. M. Weigand, “UHF RFID and tag antenna scattering—Part II: Theory,” *Microw. J.*, vol. 49, no. 6, pp. 88–92, Jul. 2006.
[18] L. Hsueh-Jyh, H.-H. Lin, and H.-H. Wu, “Effect of antenna mutual coupling on the UHF passive RFID tag detection,” presented at the IEEE Antennas and Propag. Soc. Int. Symp., 2008.
[19] F. Lu, X. Chen, and T. T. Ye, “Performance analysis of stacked RFID tags,” in *Proc. IEEE Int. Conf. on RFID*, 2009, pp. 330–337.
[20] X. Chen, F. Lu, and T. T. Ye, “The weak spots in stacked UHF RFID tags in NFC applications,” in *Proc. EEE Int. Conf. on RFID*, 2010, pp. 181–186.
[21] Y. Tanaka, Y. Umeda, O. Takyu, M. Nakayama, and K. Kodama, “Change of read range for UHF passive RFID tags in close proximity,” in *Proc. IEEE Int. Conf. on RFID*, 2009, pp. 338–345.
[22] G. Franceschetti, *Electromagnetics*. New York: Plenum Press, 1997.
[23] J. R. Mautz and R. Harrington, “Modal analysis of loaded N-port scatterers,” *IEEE Trans. Antennas Propag.*, vol. 21, no. 2, pp. 188–199, Mar. 1973.
[24] G. H. Golub and C. F. Van Loan, *Matrix Computations*, 3rd ed. Baltimore, MD: The Johns Hopkins Univ. Press, 1996.
[25] C. A. Desoer, “The maximum power transfer theorem for n-ports,” *IEEE Trans. Circuit Theory*, vol. 20, no. 3, pp. 328–330, May 1973.
[26] F. C. Chang, “Inversion of a perturbed matrix,” *Appl. Math. Lett.*, vol. 19, pp. 169–173, 2006.
[27] F. Fuschini, C. Piersanti, F. Paolazzi, and G. Falciasecca, “Analytical approach to the backscattering from UHF-RFID transponder,” *IEEE Antennas Wireless Propagat. Lett.*, vol. 7, pp. 33–35, 2008.
[28] C. Floerkemeier, R. Bhattacharyya, and S. Sarma, “Beyond the ID in RFID,” presented at the 20th Tyrrhenian Int. Workshop on Digital Communications—A CNIT Conf., Italy, 2009.
[29] G. DeJean and D. Kirovski, “Making RFIDs unique—Radio frequency certificates of authenticity,” in *Proc. IEEE Antennas and Propagation Society Int. Symp.*, Jul. 2005, vol. 1B, pp. 393–396.
[30] O. Ureten and N. Serinken, “Wireless security through RF fingerprinting,” *Can. J. Elect. Comput. Eng.*, vol. 32, no. 1, pp. 27–33, Winter, 2007.
[31] F. Broydïœ and E. Clavelier, “Taking advantage of mutual coupling in radio-communication systems using multi-port-antenna array,” *IEEE Antennas Propag. Mag.*, vol. 49, no. 4, pp. 208–220, Aug. 2007.
[32] J. W. Wallace and M. A. Jensen, “Mutual coupling in MIMO wireless systems: A rigorous network theory analysis,” *IEEE Trans. Wireless Commun.*, vol. 3, no. 4, pp. 1317–1325, Jul. 2004.

Gaetano Marrocco was born in Teramo, Italy, on August 29. 1969. He received the Laurea degree in electronic engineering and the Ph.D. in degree in applied electromagnetics from University of L'Aquila, Italy, in 1994 and 1998, respectively.

In summer 1994, he was a Postgraduate Student at the University of Illinois at Urbana Champaign. In 1997, he was appointed Researcher at the University of Rome "Tor Vergata," where he currently teaches antenna design and bioelectromagnetics. In 2010, he achieved the the rank of Associate Professor in Electromagnetics. In autumn 1999, he was a Visiting Scientist at the Imperial College in London, London, U.K. His research is mainly directed to the modeling and design of broad band and ultrawideband antennas and arrays as well as of miniaturized antennas for RFID applications. He has been involved in several space, avionic, naval and vehicular programs of the European Space Agency, NATO, Italian Space Agency, and the Italian Navy.

Dr. Marrocco currently serves as an Associate Editor of the IEEE ANTENNAS AND WIRELESS PROPAGATION LETTERS. He was the Founder and the Chair of the first two editions of the Workshop RFIDays.